ACS APPLIED MATERIALS & INTERFACES

Research Article

www.acsami.org

Molecular Weight Effect on the Efficiency of Polymer Solar Cells

Chang Liu,[†] Kai Wang,[†] Xiaowen Hu,[†,‡] Yali Yang,[§] Chih-Hao Hsu,[†] Wei Zhang,[†] Steven Xiao,[§] Xiong Gong,*[,†,‡] and Yong Cao[‡]

[†]College of Polymer Science and Polymer Engineering, University of Akron, Akron, Ohio 44325, United States

[‡]State Key Laboratory of Luminescent Materials and Devices, South China University of Technology, Guangzhou, Guangdong Province, P. R. China,

[§]1-Material Inc., 2290 Chemin St-François, Dorval, Quebec, H9P 1K2, Canada

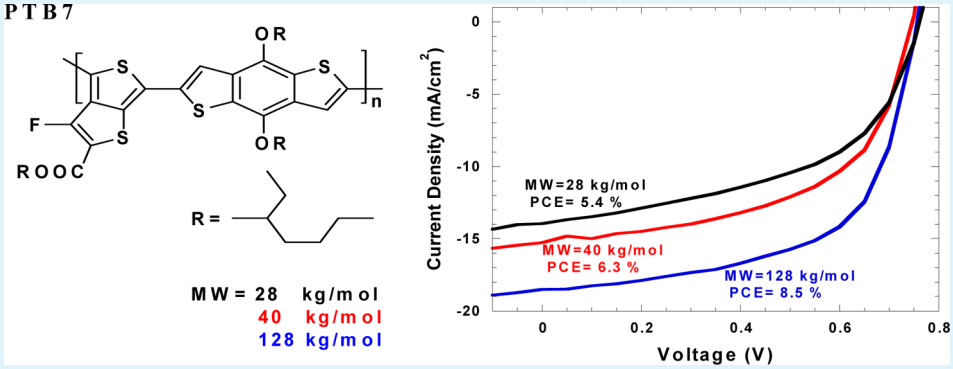

ABSTRACT: In this study, we report the investigation of the influence of molecular weight (MW) on power conversion efficiency (PCE) of bulk heterojunction (BHJ) polymer solar cells (PSCs). It was found that PCEs of PSCs fabricated by poly[[4,8-bis[(2-ethylhexyl)oxy]benzo[1,2-b:4,5-b′]dithiophene-2,6-diyl][3-fluoro-2-[(2-ethylhexyl)carbonyl]thieno[3,4-b]-thiophenediyl]] (PTB7) blended with [6,6]-phenyl-C_{71} butyric acid methyl ester ($PC_{71}BM$) as the active layer, are significantly enhanced from 5.41 to 6.27 and 8.50% along with the MW of PTB7 increased from 18 to 40 and 128 kg/mol, respectively. This enhancement is attributed to the enhanced light absorption and increased charge carrier mobility of PTB7 with high MW, and a proper phase separation in BHJ composite of PTB7:$PC_{71}BM$ interpenetrating network. All these results demonstrate that the MW of donor polymer plays an important role in the performance of BHJ PSCs.

KEYWORDS: *polymer solar cells, efficiency, molecular weight, light absorption, charge carrier mobility, phase separation*

1. INTRODUCTION

Bulk heterojunction (BHJ) polymer solar cells (PSCs) have been attracting great attention because of their advantages of flexibility, low cost, light weight, large area, clean, and processing simplicity, which make it possible to substitute its inorganic counterparts in order to finally circumvent the energy issues. Recently, 12% power conversion efficiency (PCE) of BHJ PSCs has been reported;[1] however, PSCs are still inferior to its inorganic counterparts, in term of PCE and stability. The performance of PSCs is dependent on many factors such as active layer materials, device structures, interfaces between different layers.[2] Among them, the physical properties of BHJ composites play the most important role.[3] In principal, BHJ composites demand a broad absorption response in the solar spectrum to ensure effective harvesting of solar photons. Furthermore, the energy levels of the electron donor (generally conjugated polymer) should match that of the electron acceptor (typically fullerene derivatives). That is, the donor polymer should possess a deep highest occupied molecular orbital (HOMO) to ensure a large open circuit voltage (V_{OC}), and a suitable lowest unoccupied molecular orbital (LUMO) to ensure a large energy offset between the LUMOs of donor polymer and fullerene derivative for efficient charge transport.[4] Followed above guidelines, various narrow band gap conjugated polymers have been developed so far,[5−13] among them, poly[[4,8-bis[(2-ethylhexyl)oxy]benzo[1,2-b:4,5-b′]-dithiophene-2,6-diyl][3-fluoro-2-[(2-ethylhexyl)carbonyl]-thieno[3,4-b]thiophenediyl]] (PTB7)[9] stood out as one of the most efficient narrow band gap conjugated polymers for BHJ PSCs. However, there is no report studying the influence of molecular weight (MW) of PTB7 on the device performance of PSCs based on PTB7. Studies have shown that MW of conjugated polymers can affect the effective conjugated chain length, and thus vary the optical and electric properties of conjugated polymers.[14,15] Here we report a study of the effect of the MW of PTB7 on the performance of PSCs based on PTB7:$PC_{71}BM$ ([6,6]-phenyl-C_{71}-butyric acid methyl ester)

Received: September 23, 2013
Accepted: November 1, 2013
Published: November 1, 2013

system. A solid correlation between the MW of PTB7 and PSC performances was demonstrated.

2. EXPERIMENTAL SECTION

2.1. Molecular Weight Measurement. The MW of PTB7 were determined by the Waters 2410 gel permeation chromatograph (GPC) with a refractive index detector in tetrahydrofuran (THF) using a calibration curve of polystyrene standards.

2.2. Cyclic Voltammetry. Cyclic voltammetry (CV) measurement was carried out on the BAS C3-Voltammetry Cell Stand equipped with a glassy carbon electrode as the working electrode, an Ag/Ag^+ electrode as the reference electrode, and a Pt sheet as the counter electrode. The measurements were performed in the supporting electrolyte consists of anhydrous acetonitrile (CH_3CN) mixed with tetrabutylammonium hexafluorophosphate ($((C_4H_9)_4N(PF_6))$) under an argon atmosphere with a scan rate of 100 mV/s. The potential of saturated calomel reference electrode was internally calibrated using the ferrocene/ferrocenium redox couple (Fc/Fc^+) (0.1 eV measured in the same condition), assuming an absolute energy level of −4.8 eV.

2.3. UV−Vis Absorption Spectra. The thin films of PTB7 with different MW were casted from 1,2-dichlorobenzene (*o*-DCB) solutions onto quartz glass. UV−vis absorption spectra of these thin films were measured using the HP 8453 spectrophotometer.

2.4. TEM Phase Images. Transmission electron microscope (TEM) images were obtained by using FEI-Philips scanning transmission electron microscope (Model Tecnai T12T/STEM) to observe the film morphologies of PTB7:$PC_{71}BM$ thin films.

2.5. Mobility Measurement. Space charge limited current (SCLC) method was used to estimate the hole mobility of PTB7 with different MW.[16,17] The mobility was determined by fitting the dark current observed from the hole-only diode using the single carrier SCLC model. The structure of hole-only diode was ITO/PEDOT:PSS/PTB7/MoO_3/Ag, where ITO is indium tin oxide, PEDOT:PSS is poly(3,4-ethylenedioxythiophene):poly(styrenesulfonate). PTB7 layer was casted from *o*-DCB solution. After that, MoO_3 with thickness of 10 nm and Ag with thickness of 5 nm was sequentially deposited onto top of PTB7 layer in the vacuum system with a base pressure of 4×10^{-6} mbar through a shadow mask. The device area is 0.16 cm^2.

2.6. PSCs Fabrication and Characterization. The device structure of PSCs is ITO/PEDOT:PSS/PTB7:$PC_{71}BM$/Ca/Al. The fabrication steps are as follows: patterned ITO substrates were sequentially cleaned in ultrasonic bath of detergent, deionized water, acetone, and isopropanol. Subsequently, ITO substrates were dried in oven overnight before treatment by UV-ozone for 20 min. The PTB7:$PC_{71}BM$ (PTB7:$PC_{71}BM$ = 1:1.5 by weight) BHJ composite was spin-coated onto ITO substrates from *o*-DCB solution. The thickness of PTB7:$PC_{71}BM$ was approximately 200 nm. The device fabrication was completed by thermal evaporation of 5 nm Ca coated with 100 nm Al as the cathode under vacuum with a base pressure of 4×10^{-6} mbar. The device area was 0.045 cm^2.

PSCs were characterized under an AM1.5G calibrated solar simulator (Newport model 91160−1000). The light intensity was 100 mW/cm^2. The light intensity was calibrated by utilizing a monosilicon detector (with KG-5 visible color filter) of National Renewable Energy Laboratory to reduce spectral mismatch. The current density−voltage ($J-V$) characteristics were recorded using a Keithley 2400 source meter.

3. RESULTS AND DISCUSSION

3.1. Synthesis and Characterization of PTB7. PTB7 was synthesized as reported.[18] PTB7 with different MW was obtained by Soxhlet extraction. The MW was controlled by varying the reaction time. After reaction, the mixture was added dropwise to methanol and then collected by filtration and washed with methanol. After extraction with methanol, hexane, and chloroform in Soxhlet extraction, the fraction was evaporated under reduced pressure and then precipitated in methanol, filtered, and finally dried under vacuum to obtain a dark brown solid.

The MW of PTB7 was determined by the Waters 2410 gel permeation chromatograph (GPC) with a refractive index detector in tetrahydrofuran (THF) using a calibration curve of polystyrene standards. The GPC results of these three different MW are presented in Figure 1. The MW of PTB7 was determined by GPC with the values of: 28, 40, and 128 kg/mol. The MW of PTB7 together with device performance is summarized in Table 1.

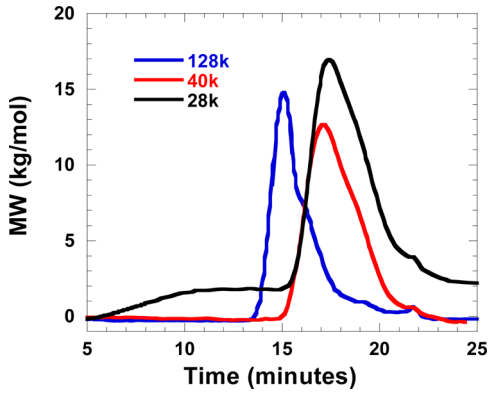

Figure 1. GPC results of PTB7 with different molecular weights.

Table 1. Molecular Weight, Optical, and Electrochemical Properties of PTB7

M_n (kg/mol)	PDI	film λ_{max} (nm)	E_g^{opt} (eV)	E_{LUMO} (eV)	E_{HOMO} (eV)	E_g^{ec} (eV)
28	1.85	673	1.66	−3.32	−5.28	1.96
40	1.54	673	1.66	−3.39	−5.28	1.89
128	1.12	677	1.62	−3.64	−5.27	1.63

3.2. Photophysical and Electrochemical Properties of PTB7. Figure 2a shows the UV absorption spectra of thin films of PTB7 with different MW. The UV absorption spectra of PTB7 with different MW were almost identical. The extinction coefficients of PTB7 show a significant effect in solid-state thin films. The film absorption coefficient continued to increase along with PTB7 MW increased from 28 to 128 kg/mol. The film absorption coefficient of PTB7 with MW of 28 kg/mol was the lowest among all the PTB7 polymers. PTB7 with low MW (28 and 40 kg/mol) have a slightly larger optical energy gap, with a 5 to 10 nm blue-shift in the absorption cutoff. The bandgap of these three polymers are 1.66, 1.66, and 1.62 eV for MW of 28, 40 kg/mol, and 128 kg/mol, correspondingly. The blue-shift in absorption spectra of PTB7 indicated less compact $\pi-\pi$ stacking in PTB7 because the main chain of PTB7 was reported to be stacked on the substrate in the face-down conformation from grazing-incidence wide-angle X-ray scattering studies.[17] Moreover, less compact $\pi-\pi$ stacking on main chain implied that charge carrier mobility of PTB7 would be small.[19]

The frontier orbital energy levels of PTB7 were obtained by using cyclic voltammetry (CV). The CV traces for PTB7 thin film referenced to ferrocene are shown in Figure 2b. The LUMO and HOMO energy levels of PTB7 are calculated through the following equations

$$E_{LUMO} = -[(E_{red} - E_{ox(Fc)} + 4.8)]\ \text{eV} \quad (1)$$

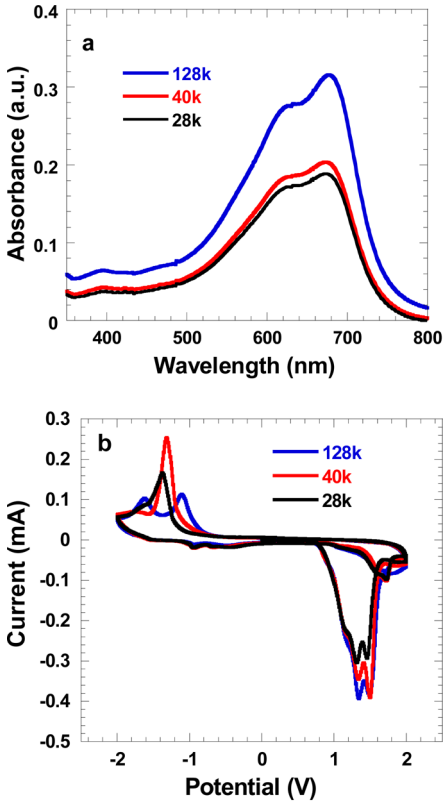

Figure 2. (a) Absorption spectra of PTB7 thin films, (b) cyclic voltammograms of PTB7 with different molecular weights.

$$E_{\mathrm{HOMO}} = -[(E_{\mathrm{ox}} - E_{\mathrm{ox(Fc)}} + 4.8)]\ \mathrm{eV} \quad (2)$$

where E_{red} is reduction potential of the polymer and E_{ox} is the oxidation potential. The HOMO and LUMO energy levels are summarized in Table 1. It was found that PTB7 with different MW possessed similar values of HOMO energy levels; however, the LUMO energy level decreased with increased MW leading to a lower bandgap for PTB7 with high MW. The lowest bandgap for PTB7 with MW of 128 kg/mol is 1.63 eV. This observation is in good agreement with the value from the optical absorption spectrum. The similar values of HOMO energy levels for PTB7 with different MW indicated a similar V_{OC} for PSCs based on PTB7 with different MW.[20]

3.3. Charge Carrier Mobility. The hole mobilities (μ_{h}) of PTB7 were estimated from the space-charge limited current (SCLC),[21] which is observed from a two-terminal diode with a structure of ITO/PEDOT:PSS/PTB7/MoO_3/Ag. The LUMO and HOMO energy levels of PTB7 and MoO_3, and the work functions of ITO, PEDOT:PSS and Ag are presented in Figure 3. According to band alignment, the electron cannot be transported from PTB7 to Ag electrode because of larger energy barrier between the LUMO energy of MoO_3 and the high work function of Ag. The $J-V$ curves and fitted lines of the diodes in the range from 0 to 4 V are shown in panels a and b in Figure 4. The hole mobility was obtained by equation

$$J = \frac{9}{8}\varepsilon_0\varepsilon_{\mathrm{r}}\mu_{\mathrm{h}}\frac{V^2}{d^3} \quad (3)$$

where ε_0 is the dielectric constant of free space, ε_{r} is the dielectric constant of the polymer. V is the voltage drop across the device, and d is the thickness of PTB7 thin film. The dielectric constant ε_{r} is assumed to be 3 in our analysis, which is

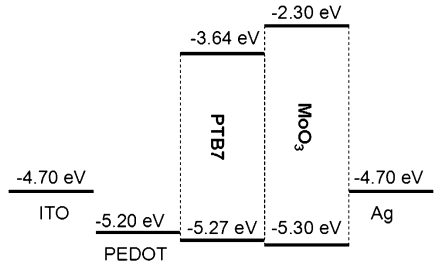

Figure 3. LUMO and HOMO energy levels of PTB7 and MoO_3, and work function of ITO and Ag.

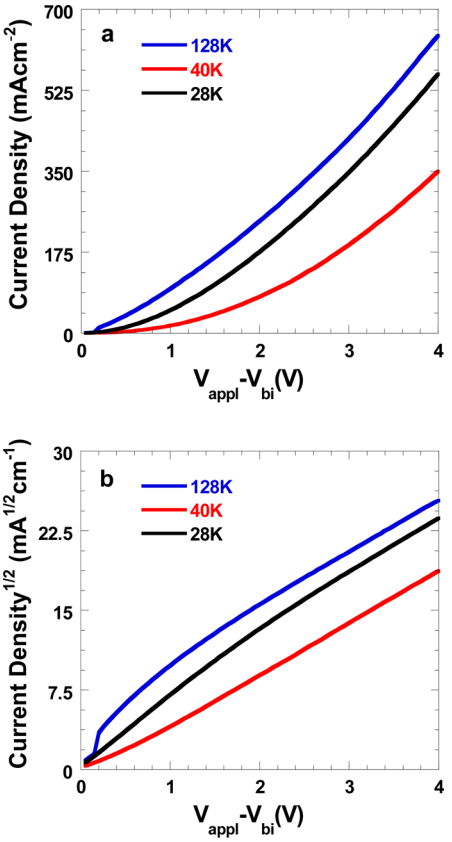

Figure 4. (a) J vs ($V_{\mathrm{appl}} - V_{\mathrm{bi}}$) and (b) $J^{1/2}$ vs ($V_{\mathrm{appl}} - V_{\mathrm{bi}}$) curves observed from the diodes with a structure of ITO/PEDOT:PSS/PTB7/MoO_3/Ag.

a typical value for conjugated polymers.[22] The thickness of PTB7 measured by AFM are 136, 176, and 180 nm for MW of 28, 40, and 128 kg/mol, respectively. The hole mobility of PTB7 are estimated to be 2.85×10^{-4} $cm^2/(V\ s)$, 4.20×10^{-4} $cm^2/(V\ s)$, 6.30×10^{-4} $cm^2/(V\ s)$ for PTB7 with a MW of 28 kg/mol, 40 kg/mol, 128 kg/mol, respectively. The change in mobilities is probably due to photoresponse limitation by confinement of conjugation length in low-molecular-weight polymers.[23] Although PTB7 with high MW probably displays a completely different structure of crystallinity, interwoven fibrils connected over long distances (ca. 500 nm),[24] leading an enhanced hole mobility.[25] Moreover, the polydispersity index (PDI) of PTB7 with MW of 128 kg/mol is only 1.12, which is much smaller than the others. Smaller PDI indicated that more regular-ordered molecular structure was formed in PTB7, which would facilitate charge transfer in comparison with PTB7 with MW of 28 and 40 kg/mol.[26]

dx.doi.org/10.1021/am404157t | ACS Appl. Mater. Interfaces 2013, 5, 12163−12167

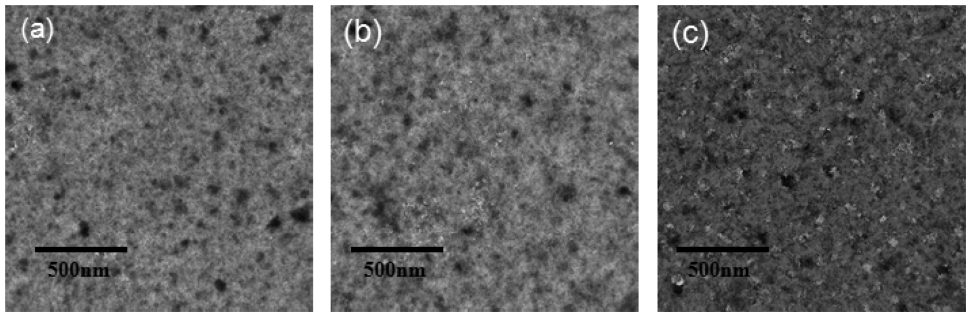

Figure 5. TEM images of PTB7:$PC_{71}BM$ BHJ composites, PTB7 with molecular weight of (a) 28, (b) 40, and (c) 128 kg/mol.

3.4. Film Morphology. To investigate the correlation between the MW and phase separation in the thin films, we carried out TEM to study the morphologies of PTB7:$PC_{71}BM$ thin films. Figure 5 presents thin film morphology of PTB7:$PC_{71}BM$ BHJ composite, where PTB7 with different MW. It was found that the phase separation from BHJ composites using PTB7 with the MW of 128 kg/mol was significantly larger than those PTB7 with low MW. The relatively larger phase separation would facilitate charge separation and transport within BHJ composite.[27] As a result; better device performance is anticipated from PSCs based on PTB7 with high MW.[28]

3.5. Photovoltaic Properties. The effect of MW on the photovoltaic properties of PTB7 was investigated using a device configuration of ITO/PEDOT:PSS/PTB7:$PC_{71}BM$/Ca/Al. The $J-V$ curves of BHJ PSCs are shown in Figure 6a. Under AM1.5G illumination with the light intensity of 100 mW cm^{-2}, a V_{OC} of 0.76 V, a J_{SC} of 18.51 $mAcm^{-2}$, a fill factor (FF) of 60%, and a corresponding PCE of 8.50% were obtained from PSCs by using PTB7 with MW of 128 kg/mol. Under the same condition, a V_{OC} of 0.76 V, a J_{SC} of 15.27 mA cm^{-2}, a FF of 54%, and a corresponding PCE of 6.27% were observed from PSCs by using PTB7 with MW of 40 kg/mol. For PSCs using PTB7 with MW of 28 kg/mol, a V_{OC} of 0.75 V, a J_{SC} of 13.96 mA cm^{-2}, a FF of 52%, and a corresponding PCE of 5.41% were observed. The similar V_{OC} observed from PSCs based on PTB7 with different MW is consistent with the HOMO energy levels of PTB7. A significant increased J_{SC} was observed from PSCs using PTB7 with high MW. Overall, It was clearly that the MW of PTB7 played an important role in the device performance.

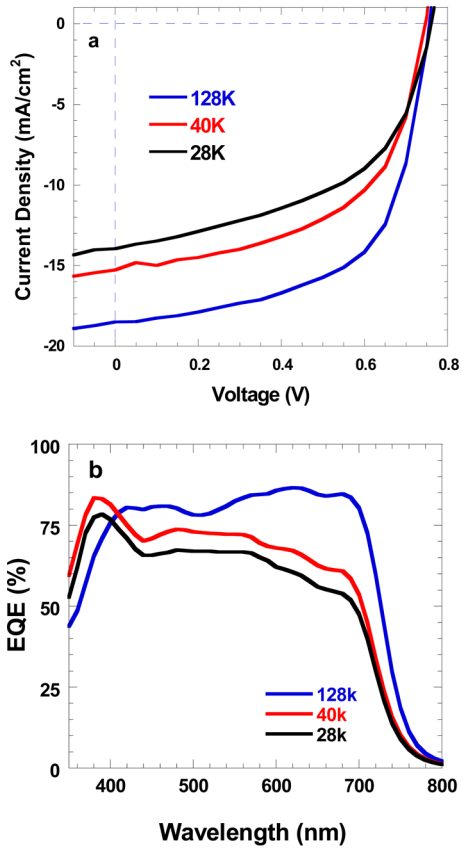

Figure 6. (a) $J-V$ curves of PSCs, (b) EQE of PSCs.

As discussed above, the difference among PTB7 with different MW is their absorption spectra (Figure 2a) and hole mobilities (Figure 4), the difference among PTB7:$PC_{71}BM$ BHJ composites is their phase separation morphologies (Figure 5). Therefore, enhanced absorption efficiency and increased hole mobility of PTB7 with high MW and a proper phase separation of PTB7:PCBM are responsible for enlarged J_{SC} and FF.

To further understand underlying increased efficiency from PSCs using PTB7 with high MW, the external quantum efficiencies (EQE) of PSCs were measured and compared. Figure 6b presents the EQEs of PSCs using PTB7 with different MW. The EQE ranging from 350 to 800 nm is in good agreement with absorption spectra of PTB7 (Figure 2a) with different MW. However, increased EQEs from PSCs using PTB7 with high MW indicated that high hole mobility of PTB7 with high MW and a proper phase separation of BHJ are contributed to enlarged J_{SC} and FF.

4. CONCLUSION

The device performance of polymer solar cells influenced by the polymer with different molecular weight was investigated. Strong correlations between the molecular weight and thin film absorption, charge carrier mobilities, film morphologies and photovoltaic performances were demonstrated. We found that efficiency of polymer solar cells is significantly enhanced from 5.41 to 6.27 and 8.50% when the molecular weights of donor polymer PTB7 is increased from 28 to 40 and 128 kg/mol, respectively. These results demonstrated the importance of achieving high molecular weight in the design of semiconducting polymers plays an important role in achieving high performance of PSCs.

AUTHOR INFORMATION

Corresponding Author

*E-mail: e-mail:xgong@uakron.edu. Fax: (330) 972-3406.

Notes

The authors declare no competing financial interest.

ACKNOWLEDGMENTS

The work was partially supported by 3M Company. X.W.H. thanks the China Scholarship Council for the Joint Ph. D. program. The authors at SCUT thank NSFC for financial support (51329301).

REFERENCES

(1) Heo, J. H.; Im, S. H.; Noh, J. H.; Mandal, T. N.; Lim, C. S.; Chang, J. A.; Lee, Y. H.; Kim, H. J.; Sarkar, A.; Nazeeruddin, M. K.; Gratzel, M.; Seok, S. *Nat. Photonics* **2013**, *80*, 1−6.
(2) Dennler, G.; Scharber, M. C.; Brabec, C. J. *Adv. Mater.* **2009**, *21*, 1323−1338.
(3) Li, G.; Shrotriya, V.; Yao, Y.; Huang, J. S.; Yang, Y. *J. Mater. Chem.* **2007**, *17*, 3126−3140.
(4) Thompson, B. C.; Fréchet, J. M. J. *Angew. Chem., Int. Ed.* **2008**, *47*, 58−77.
(5) Chen, H. Y.; Hou, J.; Zhang, S.; Liang, Y.; Yang, G.; Yang, Y.; Yu, L.; Li, G. *Nat. Photonics* **2009**, *3*, 649−653.
(6) Bundgaard, E.; Krebs, F. C. *Sol. Energy Mater. Sol. Cells* **2007**, *11*, 954−985.
(7) Winder, C.; Sariciftci, N. S. *J. Mater. Chem.* **2004**, *14*, 1077−1086.
(8) Cheng, Y.; Yang, S.; Hsu, C. *Chem. Rev.* **2009**, *109*, 5868−5923.
(9) Liang, Y.; Xu, Z.; Xia, J.; Tsai, S. T.; Wu, Y.; Li, G.; Ray, C.; Yu, L. *Adv. Mater.* **2010**, *22*, E135−E138.
(10) Carsten, B.; Szarko, J. M.; Son, H. J.; Wang, W.; Lu, L.; He, F.; Rolczynski, B. S.; Lou, S. J.; Chen, L. X.; Yu, L. *J. Am. Chem. Soc.* **2011**, *133*, 20468−20475.
(11) Li, Y. *Acc. Chem. Res.* **2012**, *45*, 723−733.
(12) Thompson, B. C.; Frechet, J. M. J. *Angew. Chem., Int. Ed.* **2008**, *47*, 58−77.
(13) Shieh, J. T.; Liu, C. H.; Meng, H. F.; Tseng, S. R.; Chao, Y. C.; Horng, S. F. *J. Appl. Phys.* **2010**, *107*, 084503.
(14) Yiu, A. T.; Beaujuge, P. M.; Lee, O. P.; Woo, C. J.; Toney, M. F.; Fréchet, J. M. J. *J. Am. Chem. Soc* **2012**, *134*, 2180−2185.
(15) Saka, I.; Shimawaki, M.; Mori, H.; Doi, I.; Miyazaki, E.; Koganezawa, T.; Takimiya, K. *J. Am. Chem. Soc.* **2012**, *134*, 3498−3507.
(16) Li, G.; Shrotriya, V.; Yao, Y.; Huang, J. S.; Yang, Y. *J. Mater. Chem.* **2007**, *17*, 3126−3140.
(17) Mihailetchi, V. D.; Koster, L. J. A.; Blom, P. W. M.; Melzer, C.; De Boer, B.; Van Duren, J. K.; Janssen, R. A. J. *Adv. Funct. Mater.* **2005**, *15*, 795−801.
(18) Son, H. J.; Wang, W.; Xu, T.; Liang, Y. Y.; Wu, Y.; Li, G.; Yu, L. *J. Am. Chem. Soc.* **2011**, *133*, 1885−1894.
(19) Egbe, D. A. M.; Türk, S.; Rathgeber, S.; Kühnlenz, F.; Jadhav, R.; Wild, R.; Birckner, E.; Adam, G.; Pivrikas, A.; Cimrova, V.; Knör, G.; Sariciftci, N. S.; Hoppe, H. *Macromolecules* **2010**, *43*, 1261−1269.
(20) Joa, M. Y.; Parka, S. J.; Park, T.; Wonc, Y. S.; Kim, J. H. *Org. Electron.* **2012**, *13*, 2185−2191.
(21) He, Z.; Zhong, C.; Su, S.; Xu, M.; Wu, H.; Cao, Y. *Nat. Photonics* **2012**, *6*, 591−595.
(22) Campbell, I. H.; Hagler, T. W.; Smith, D. L. *Phys. Rev. Lett.* **1996**, *76*, 1900−1903.
(23) Zhang, R.; Li, B.; Iovu, M. C.; Jeffries-EL, M.; Sauve, G.; Cooper, G.; Jia, S.; Tristram-Nagle, S.; Smilgies, D. M.; Lambeth, D. N.; McCullough, R. D.; Kowalewski, T. *J. Am. Chem. Soc.* **2006**, *128*, 3480−3481.
(24) Osipov, M. A. In *Handbook of Liquid Crystals*, 1st ed.; Demus, D., Goodby, J., Gray, G. W., Spiess, H. W., Vill, V., Eds.; Wiley-VCH: Weinheim, Germany, 1998; Vol. 3, p 41.
(25) Ballantyne, A. M.; Chen, L.; Dane, J.; Hammant, T.; Braun, F. M.; Heeney, M.; Duffy, W.; McCulloch, I.; Bradley, D. D. C.; Nelson, J. *Adv. Funct. Mater.* **2008**, *18*, 2373−2380.
(26) Hiorns, R. C.; Bettignies, R.; Leroy, J.; Bailly, S.; Firon, M.; Seintein, C.; Khoukh, A.; Preud'homme, H.; Dagron-Lartigau, C. *Adv. Funct. Mater.* **2006**, *16*, 2263−2273.
(27) Yang, X. N.; Loos, J.; Veenstra, S. C.; Verhees, W. J. H.; Wienk, M. M.; Kroon, J. M.; Michels, M. A. J.; Janssen, R. A. J. *Nano Lett.* **2005**, *5*, 579−583.
(28) Hoven, C. V.; Dang, X. D.; Coffin, R. C.; Peet, J.; Nguyen, T. Q.; Bazan, G. C. *Adv. Mater.* **2010**, *22*, E63−E66.